J. Appl. Comput. Mech., 5(5) (2019) 900-917
DOI: 10.22055/JACM.2019.27857.1439

ISSN: 2383-4536
jacm.scu.ac.ir

M&MoCS
Shahid Chamran University of Ahvaz

Journal of Applied and Computational Mechanics

Research Paper

Vibration and Buckling Analysis of Functionally Graded Flexoelectric Smart Beam

Milad Esmaeili, Yaghoub Tadi Beni

Mechanical Engineering Department, Faculty of Engineering, Shahrekord University, Shahrekord, Iran

Received December 11 2018; Revised March 18 2019; Accepted for publication April 06 2019.
Corresponding author: Y.T. Beni, tadi@eng.sku.ac.ir

Abstract: In this paper, the buckling and vibration behaviour of functionally graded flexoelectric nanobeam is examined. The vibration and buckling formulations of functionally graded nanobeam are developed by using a new theory that's presented exclusively for flexoelecteric nano-materials. So by considering Von-Karman strain and forming enthalpy equation based on displacement, polarization and electric potential, electromechanical coupling equations are developed base on Hamilton' principle. By considering boundary condition of simply support and clamped-clamped and also Euler-Bernoulli beam model, pre-buckling, buckling and the vibration behavior of functionally graded nanobeam affected by flexoelectric will be investigated.

Keywords: Flexoelectric effect, Functionally graded nanobeam, Piezoelectric effect, Size-dependent, Euler-Bernoulli beam model.

1. Introduction

Beams play an important role in mechanical and electromechanical systems such as sensors and actuators. They are often exposed to dynamic and static stimulation. Vibrations and natural frequencies and buckling are important subjects in beam analysis. Many studies have been done on natural frequency and critical buckling load.

Because of commercial uses of micro-electromechanical systems (MEMs) and nano-electromechanical systems (NEMs), they have been studied in recent decades [1]. For example, recently electromechanical mirrors for light switches have revolutionized communication industry [2]. Todays, micro/nano systems have important position in many scientific and industrial areas. Most of systems operate based on vibration and beam deflection in micro/ nano dimensions; so study and control of micro/nano beams behavior is of great importance. Among micro/ nano particles, clamped- clamped beams by using electrostatic or piezoelectric stimulation have great usages. For example, cantilever beams have been used in atomic microscopes, microswitches and accelerometers, and clamped-clamped beams used in micromirrors.

Normal dimensions of microelectromechanical systems are some micrometers to hundred of micrometers. Technological importance of microelectromechanical systems are not only limited to their sizes but also it's because of their usage in technologies of flat processing in integrated electric circuits and also their simultaneous use with so many partially simple mechanical systems. Nanoelectromechanical systems are shown with their small dimensions. These dimensions are related to systems operation. Critical sizes may be hundreds or a few nanometers. New physical characteristics that derived from small dimension coped with systems operation so it's possible to need a new model.

For finding a solution to understand the importance of nanotechnology in beams we should know them. Nano and micro beams are widely used in systems and nano and micro sized devices like biosensors, nanowires, atomic microscopes, microstimulators, films with a few thicknesses and microelectromechanical and nanoelectromechanical systems. It's not easy to design and analyze these systems and machines because electromechanical problems are generally nonlinear and secondly important phenomena like pull-in instability, electromechanical buckling, dynamic buckling, vibration and other problems and related design should be searched.

Piezoelectric has capability of changing mechanical energy to electric energy and vice versa. When a piezoelectric material is exposed to stress or mechanical pressure, proportion to this pressure, an electric potential will produce that's called direct piezoelectric effect. So if piezoelectric material is exposed to electric field, proportion to this field, a mechanical deflection will happen, that's call inverse piezoelectric [3].

Piezoelectric is well investigated in bulk materials and recently it has been noted in nanomaterials. For showing anisotropic characteristics like piezoelectricity, materials should not center of symmetry. 21 crystals of 32 known crystals don't have center of symmetry and 20 of these 21 crystals have piezoelectric characteristic in their longitudinal axis. 10 of these 21 crystals have only one longitudinal axis that are called polarized crystals and have self-polarized characteristics. This self-polarized characteristics depend on temperature and in fact temperature leads to electric pole in material and is known as pyroelectricity. Crystals with pyroelectric characteristics by exposing to electric field will decrease or fade their self-polarized effect and called ferroelectric crystals [4].

Common electromechanical coupling between electric polarization and stable strain is unique for noncentrosymmetric crystalslike piezoelectric material [5]. Although presence of a strain gradient or non-uniform strain function can disturb inverse symmetry, and produce an electric polarization even in dielectric centrosymmetric crystals [6]. This auto electric polarization that's caused by strain gradient called flexoelectricity that is proportioned with flexoelectric coefficient and the amount of strain gradient. It's expected that flexoelectricity be weaker than piezoelectricity however it's possible to have a striking role in nanoscale because of the fact that strain gradient has an inverse proportion with scale structure characteristics [7].

So, it's necessary to consider the flexoelectric effect on studying electromechanical coupling in dielectric. Recently flecxoelectric leads to an increase in scientific interests and research activities. A special use of flexoelectricity has been focused on structuring piezoelectric nano-materials without piezoelectric materials [8, 9].

Findings show that flexoelectric effect plays an important role in physical characteristics of ferroelectrics such as dielectric constants [10], the polarization hysteresis curves [11], critical thickness of films in which automatic changeover polarization will fade [12] and critical transition temperature of nanowires and thin plates [13].

Recently functionally graded materials have an increasing usage in micro and nano structures, such as thin films in form of memory alloys [14, 15]. Feo et al. [16], Lee et al. [17] and Vittorio et al. [18], investigated the functionally graded materials in micro electromechanical and nano electromechanical systems. So a lot of researchers focused on investigating the static and dynamic behavior of functionally graded beam in both MEMS and NEMS.

Ma and Cross [19-22] have made different experiments for measuring flexoelectric coefficient in some of dielectricxs. Reports show that big and tangible flexoelectric coefficients are suited for high flexible ferroelectrics. In contrast, it's estimated that flexoelectric constants are some order less than measurements of atomic stimulations [23, 24].

Lately, Ponomareva et al. have studied this subject [25], by the fact that flexoelectric coefficient is temperature dependent. Some efforts have been done for setting a theoretical framework for dielectrics by considering flexoelectric effects, to quantitatively understand the basic physics of electromechanical coupling of dielectrics in nanoscale.

Findings show that there's a direct relationship between mechanical and electric characteristics of nanoscale piezoelectric and flexoelectric material with size effect [26-28]. Besides, by using size dependent theories, researchers studied the relationship between flexoelectric and piezoelectric beams and found their mechanical and electric characteristics [26, 29].

By using Euler-Bernoulli beam model, Kong et al. investigated free vibration microbeams affected by size parameters by modified couple stress theory and used boundary value for solving equations. Results show that by considering size effect, natural frequency is more than the amount obtained by classical theory [30].

Sadeghi et al. investigated the effect of small size on bending, vibrations and stability of functionally graded microbeams by strain gradient theory [31]. Zhi Yan et al. investigated the effect of flexoelectric on static buckling and free vibration of a simply support piezoelectric nanobeam based on generalized linear theory of piezoelectricity and Timoshenko beam model [32]. It's found that flexoelectricity has a striking effect on beam deflection and it's possible to inverse deflection direction on a distinct loading condition. It's shown that frequency allocation for piezoelectric nanobeam should be mixed with flexoelectric effect (that's obtained by exposing electric load) [32].

Liang and Shen investigated the buckling and vibration of piezoelectric nanostructures affected by flexoelectric. In piezoelectric nano structures, there's always a discussion on surface value, length and effect of electric load production on critical buckling and in this research they showed that flexoelectric has a determining role on sensitivity to voltage change in nanobeams and critical buckling [33]. Zhiang et al. discussed the effect of flexoelectric on hollow nano cylinder. They connected the outlet voltage of voltmeter to internal surface of cylinder and its external surface, and measured the amount of received voltage in voltmeter, critical buckling and its sensitivity by changing hydrostatic and electric mechanical load [34]. Kundalwal and Meguid investigated the effect of carbon nanotube (CNT) waviness on the active constrained layer damping (ACLD) of the laminated fuzzy fiber-reinforced composite (FFRC) shells [35]. Their results show that, the planar orientation of CNT waviness has a significant influence on the damping characteristics of the laminated FFRC shells and damping characteristics of the symmetric cross-ply, and antisymmetric angle-ply laminated FFRC shells are improved if CNT waviness is coplanar with the longitudinal plane of the carbon fiber [35]. Kundalwal et al. examined the investigation of active constrained layer damping of smart laminated continuous fuzzy fiber reinforced composite shells [36]. Suresh Kumar et al. investigated the controlling of the large amplitude vibrations of doubly curved sandwich shells with facings composed of FFRC [37]. Kundalwal et al. developed finite element models to predict the effective piezoelectric and elastic properties of the graphene reinforced nanocomposite material (GRNC) based on the linear piezoelectricity and Euler beam theories [38]. Kundalwal et al. showed that the strain gradient in non-piezoelectric graphene sheet affected the ionic positions and the asymmetric redistribution of the electron density [39].

Chu et al. studied the static bending and free vibration of flexoelectric functionally graded nanobeams with general modified strain gradient theory. Numerical results indicate that flexoelectric effect can observably influence the electromechanical response in functionally graded piezoelectric nanobeam at nanometer scale [40].

There are more research in the literature about the analysis of flexoelectric nano/micro structures by using the finite element method [41-45]. Wei et al. investigated the size-dependent mechanical properties of nanostructures with the finite element method by developing a kind of surface element to take the surface elastic effect [41]. T. Darrall et al. develop the finite element variational formulation upon a recent consistent size-dependent theory that incorporates the interactions between the electric field and the mechanical mean curvatures in dielectrics, including those with centrosymmetric structure [42]. Shijie et al. utilized an iterative finite element algorithm to investigate the size-dependent Euler–Bernoulli beam model, which takes the flexoelectricity, piezoelectricity, and dielectricity as well as the surface elasticity theory [43].

One of the important application of flexoelectric nanobeam is in the energy harvester. Recently, researchers try modeling the flexoelectric harvester process. Moura and Erturk used electroelastodynamic framework to analysis the flexoelectric energy harvesting from strain gradient fluctuations in centrosymmetric dielectrics. The flexoelectric energy harvester model is based on the Euler-Bernoulli beam theory and it assumes the main source of polarization to be static bulk flexoelectricity [46]. Liang et al. developed mechanical energy harvester models on Timoshenko laminated beam theory, in which the flexoelectric and piezoelectric mechanisms were discussed. The energy conversion calculated for different numbers of layers also indicates that laminated energy harvester systems excel single-layered energy harvesters [47]. Liang et al. also established theoretical framework to investigate the circuit voltage, electric power of nanoscale mechanical energy harvesting, in which the mechanical vibration energy was converted into electrical energy by piezoelectric and flexoelectric effects [48]. Deng et al. investigated the possibility of using the phenomenon of flexoelectricity for energy harvesting. The flexoelectric effect is universally present in all dielectrics and exhibits a strong scaling with size. They theoretically and computationally examined flexoelectric energy harvesting under harmonic mechanical excitation [49]. Wang and Wang investigated a theoretical model incorporating flexoelectricity and piezoelectricity for energy harvesting. Their model includes geometric nonlinearity deformation and damping effect so that it can more accurately predict the electromechanical behavior of energy harvesters [50].

It's clear from above discussion that flexoelectric effect has great importance a scale of nano, and by increasing researches about replacement of flexoelectric materials with piezoelectric materials, we can conclude that flexoelectric effect should be investigated. On the other hand, investigation of mechanical properties on nanobeams as the main element of nanostructures has a great importance, In this paper by using Euler-Bernoulli beam model some mechanical properties such as vibration and buckling of functionally graded nanobeam are investigated. For doing our research governing equations are derived by Hamilton's principle. Then geometric and material (electromechanical) parameters on buckling behavior and nanobeam vibration will investigate.

2. Preliminaries

In an extended linear theory for dielectrics [6, 51], general expression of internal energy function is not only related to strain and polarization but also to their gradients.

$$U = U\left(\varepsilon_{ij}, \eta_{ijk}, P_i, Q_{ij}\right) \tag{1}$$

That, in this relation ε_{ij} is symmetric tensor of classic strain and $\eta_{ijk} = \varepsilon_{jk,i}$ is strain gradient tensor and P_i is polarization vector and $Q_{ij} = P_{i,j}$ is polarization gradient tensor. Classic strain tensor defined as:

$$\varepsilon_{ij} = \frac{1}{2}(u_{i,j} + u_{j,i}) \tag{2}$$

That u_i in relation (2) is displacement field. In derivation of relation by Maranganti et al. and Shen and Hu, equations of internal energy density are [6, 52]:

$$\sigma_{ij} = \frac{\partial U}{\partial \varepsilon_{ij}}, \tau_{ijk} = \frac{\partial U}{\partial \eta_{ijk}}, E_i = \frac{\partial U}{\partial P_i}, V_{ij} = \frac{\partial U}{\partial Q_{ij}} \quad (3)$$

That σ_{ij} is stress tensor, E_i is local effective electric field, τ_{ijk}, V_{ij} are higher-order stress and higher- order local electric field respectively. By using relation (3), internal energy density can express as [53]:

$$U = \frac{1}{2}\left(\sigma_{ij}\varepsilon_{ij} + \tau_{ijk}\eta_{ijk} + E_i P_i + V_{ij}Q_{ij}\right) \quad (4)$$

Besides, electric enthalpy density is divided to internal energy density and remaining by Toupin [54]. By developing electric enthalpy density that included flexoelectricity, electric enthalpy density H is shown as:

$$H = U - \frac{1}{2}\varepsilon_0\varphi_{,i}\varphi_{,i} + \varphi_{,i} P_i \quad (5)$$

In which ε_0 is vaccum permittivity and φ is Maxwell self-field. Maxwell self-field is defined as:

$$E_i^{MS} = -\varphi_{,i} \quad (6)$$

Also electrostatic stress σ_{ki}^{ES} is generally defined as:

$$\sigma_{ki}^{ES} = -V_{ji}P_{j,k} + \frac{1}{2}\left(\sigma_{lj}\varepsilon_{lj} + \tau_{lst}\eta_{lst} + E_j P_j + V_{lj}Q_{lj}\right)\delta_{ik} - D_i\varphi_{,k} + \left(-\frac{1}{2}\varepsilon_0\varphi_{,j}\varphi_{,j} + \varphi_{,j} P_j\right)\delta_{ik} \quad (7)$$

In above equation, D_i is electric displacement and expressed as:

$$D_i = -\varepsilon_0\phi_{,i} + P_i \quad (8)$$

In relation (7), $\sigma_{lj}\varepsilon_{lj}$ and $\tau_{lst}\eta_{lst}$ can be avoided because of small amount of strain value. On the one hand, by using Reynolds transport theorem [55], variation of general enthalpy for a flexoelectric structure is:

$$\delta\int_V HdV = \int_V \delta HdV + \int_V H\delta u_{k,k}dV \quad (9)$$

Also, kinetic energy of a continuous nanobeam is calculated by this relation:

$$\mathrm{K} = \int \frac{1}{2}\rho\left(\bar{z}\right)\left(\dot{u}_1^2 + \dot{u}_2^2 + \dot{u}_3^2\right)\mathrm{dV} \quad (10)$$

That ρ is nanobeam density. At last, Hamilton's principle is used for deriving equations that's expressed as:

$$\delta\int_{t_1}^{t_2}\left(-\int_V HdV + K + W\right)dt = 0 \quad (11)$$

That W is work of external forces. In this paper, presented theory for flexoelectric materials by Li et al. [53] for derivation of equations is used. According to this theory, relation of strain energy density is as below:

$$U = \frac{1}{2}\left(\sigma_{ij}\varepsilon_{ij} + p_i\gamma_i + \tau_{ijk}^{(1)}\eta_{ijk}^{(1)} + m_{ij}^{'}\chi_{ij}^{'} + E_i P_i + V_{ij}Q_{ij}\right) \quad (12)$$

where, p_i, $\tau_{ijk}^{(1)}$, $m_{ij}^{'}$ are components of higher-order stresses and γ_i, $\eta_{ijk}^{(1)}$, $\chi_{ij}^{'}$ are dilatation gradient, deviatoric stretch gradient and deviatoric rotation gradient. Constitutive relations for flexoelectric materials are [53]:

$$\sigma_{ij} = k\delta_{ij}\varepsilon_{nn} + 2\mu\varepsilon_{ij}^{'} - f_1\delta_{ij}Q_{kk} - 2f_2Q_{ij} \quad (13)$$

$$p_i = 2\mu l_0^2 \gamma_i + \left(f_1 + \frac{2}{3} f_2 \right) P_i \tag{14}$$

$$\tau_{ijk}^{(1)} = 2\mu l_1^2 \eta_{ijk}^{(1)} \tag{15}$$

$$m_{ij}^{'} = 2\mu \left(l_2^2 + \frac{9}{5} l_0^2 \right) \chi_{ij}^{'} + 2\mu \left(l_2^2 - \frac{9}{5} l_0^2 \right) \chi_{ji}^{'} + 2 f_2 e_{ijk} P_k \tag{16}$$

$$E_i = \alpha P_i + \left(f_1 + \frac{2}{3} f_2 \right) \gamma_i + 2 f_2 e_{ijk} \chi_{jk}^{'} \tag{17}$$

$$V_{ij} = \alpha \left(\delta_{ij} \beta_1^2 Q_{nn} + \beta_2^2 Q_{ij} + \beta_3^2 Q_{ji} \right) - f_1 \delta_{ij} \varepsilon_{nn} - 2 f_2 \varepsilon_{ij} \tag{18}$$

In above relations, $l_i\left(i = 0,1,2\right)$, $\beta_i\left(i = 1,2,3\right)$ are size effect parameters that related to length dimensions of strain gradient and polarization gradient, respectively. k is bulk modulus, μ is Lame constant. f_1 and f_2 are flexoelectric coefficients and α is reciprocal dielectric susceptibility and δ is kronecker delta and e_{ijk} is the symbol of permutation.

Deviatoric strain tensor components and dilatation gradient and deviatoric stretch gradient and deviatoric rotation gradient are obtained by:

$$\varepsilon_{ij,k}^{'} = \varepsilon_{ij,k} - \frac{1}{3} \delta_{ij} \varepsilon_{nn,k} \tag{19}$$

$$\gamma_i = \varepsilon_{nn,i} \tag{20}$$

$$\eta_{ijk}^{(1)} = \eta_{ijk}^{(s)} - \eta_{ijk}^{(0)} \tag{21}$$

$$\eta_{ijk}^{(0)} = \frac{1}{5} \left(\delta_{ij} \eta_{mmk}^{(s)} + \delta_{jk} \eta_{mmi}^{(s)} + \delta_{ki} \eta_{mmj}^{(s)} \right) \tag{21a}$$

$$\eta_{ijk}^{(s)} = \frac{1}{3} \left(\varepsilon_{jk,i} + \varepsilon_{ki,j} + \varepsilon_{ij,k} \right) \tag{21b}$$

$$\chi_{ij}^{'} = e_{ipq} \eta_{pqj}^{'} \tag{22}$$

$$\eta_{ijk}^{'} = \varepsilon_{kj,i}^{'} \tag{23}$$

3. Governing Equations of Functionally Graded Flexoelectric Nanobeam

For obtaining beams equations by Euler-Bernoulli beam model, a displacement field according to Euler-Bernoulli beam's model should be considered. The displacement field is:

$$\begin{aligned} u_1\left(x,z,t\right) &= u_0\left(x,t\right) - z \frac{\partial w\left(x,t\right)}{\partial x} \\ u_2 &= 0 \\ u_3 &= w\left(x,t\right) \end{aligned} \tag{24}$$

where, u_0 and w are displacements of every point in the beam neutral axis in x and z axis direction, respectively. According to relation (2), the nonzero strain tensor component by considering displacement field and nonlinear Von Karman strain is calculated by:

$$\varepsilon_{11}=\frac{\partial u_0(x,t)}{\partial x}-z\frac{\partial^2 w(x,t)}{\partial x^2}+\frac{1}{2}\left(\frac{\partial w}{\partial x}\right)^2 \tag{25}$$

Foe calculating material properties of functionally graded beam, it is supposed that mechanical properties will change in z axis and second for calculating these mechanical properties, the place of neutral axis should be found. That according to figure (1), $\bar{z}$ is the distance of arbitrary point from the bottom surface and $\overline{z_c}$ is the distance of neutral axis from bottom surface. If the left side of the beam is immovable and the right-hand side is movable, equilibrium equation in a longitudinal direction will be used for finding the location neutral axis [40]. Like this:

$$\int \sigma_{11}^0 dA=0 \tag{26}$$

It should be noted that σ_{11}^0 is axial stress that's produced by initial strain and it's only calculated in bending conditions. Finally, equilibrium equation (26) lead to finding the location of neutral axis as:

$$\overline{z_c}=\frac{\int E(\bar{z})\bar{z}dA}{\int E(\bar{z})dA} \tag{27}$$

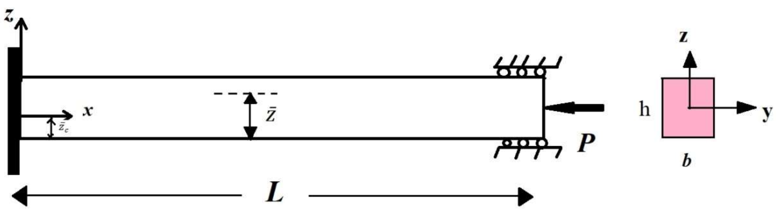

Fig. 1. Schematic view of flexoelectric nanobeam

By using Hamilton's principle in (11) and doing variation operations for all displacement components, after doing long mathematical calculation, nanobeam equations can be express as following:
Equation of motion in longitudinal direction of beam is:

$$-\frac{\partial}{\partial x}\left(N+N^{ES}\right)+\frac{\partial^2}{\partial x^2}\left(N^h\right)+K_{11}\frac{\partial^2 u_0}{\partial t^2}-L_{11}\frac{\partial^3 w}{\partial x\partial t^2}=0 \tag{28}$$

Related boundary conditions are as following:

$$\left(N^h\right)\frac{\partial \delta u_0}{\partial x}\bigg|_0^L=0 \quad , \quad \left(N-\frac{\partial}{\partial x}\left(N^h\right)-\bar{N}\right)\delta u_0\bigg|_0^L=0 \tag{29}$$

Also, equation of motion in the horizontal direction of beam:

$$\frac{\partial^3}{\partial x^3}\left(M^h\right)+\frac{\partial^2}{\partial x^2}\left(-M-M^{ES}+\left(N^h\right)\frac{\partial w}{\partial x}\right)+\frac{\partial}{\partial x}\left(-N\frac{\partial w}{\partial x}+\left(-N^h\right)\frac{\partial^2 w}{\partial x^2}\right)+(K_{11})\frac{\partial^2 w}{\partial x^2}-(M_{11})\frac{\partial^4 w}{\partial x^2\partial t^2}+\left(L_{11}\right)\frac{\partial^3 u_0}{\partial x\partial t^2}=0 \tag{30}$$

Related boundary conditions are as following:

$$\left(-M^h\right)\frac{\partial^2 \delta w}{\partial x^2}\bigg|_0^L=0 \quad ,\left(-M-M^{ES}+\frac{\partial}{\partial x}\left(M^h\right)+\left(N^h\right)\frac{\partial w}{\partial x}\right)\frac{\partial \delta w}{\partial x}\bigg|_0^L=0$$

$$\left[\frac{\partial^2}{\partial x^2}\left(-M^h\right)+\frac{\partial}{\partial x}(M)+\left(\left(N^h\right)\frac{\partial^2 w}{\partial x^2}\right)+\frac{\partial}{\partial x}\left(-N^h\frac{\partial w}{\partial x}\right)+N\frac{\partial w}{\partial x}\right]\delta w\bigg|_0^L=0 \tag{31}$$

For a beam with a width of b, axial stress resultant N, the moment resultant M, higher-order axial stress resultant N^h, higher-order moment resultant M^h are defined respectively as below:

$$N = b\int_{-\bar{z}_c}^{h-\bar{z}_c} (\sigma_{11})\,dz$$

$$M = b\int_{-\bar{z}_c}^{h-\bar{z}_c} \left(z(\sigma_{11}) + p_3 + \tau_{113}^{(1)} + \frac{2}{3}m'_{21} + \frac{1}{3}m'_{12} \right) dz$$

$$N^h = b\int_{-\bar{z}_c}^{h-\bar{z}_c} \left(p_1 + \tau_{111}^{(1)} + \frac{1}{3}m'_{23} - \frac{1}{3}m'_{32} \right) dz$$

$$M^h = b\int_{-\bar{z}_c}^{h-\bar{z}_c} z\left(p_1 + \tau_{111}^{(1)} + \frac{1}{3}m'_{23} - \frac{1}{3}m'_{32} \right) dz \tag{32}$$

$$N^{ES} = b\int_{-\bar{z}_c}^{h-\bar{z}_c} \left(\sigma_{11}^{ES}\right) dz \quad , M^{ES} = b\int_{-\bar{z}_c}^{h-\bar{z}_c} z\left(\sigma_{11}^{ES}\right) dz$$

That K_{11}, L_{11}, M_{11} are defined as following:

$$\left(K_{11}, L_{11}, M_{11}\right) = b\int_{-\bar{z}_c}^{h-\bar{z}_c} \rho\left(\bar{z}\right)(1, z, z^2)\,dz \tag{33}$$

Also, after simplification of δP_3 and $\delta\varphi$, there are two electric equations with their boundary conditions as following:

$$E_3 - V_{33,3} + \frac{d\varphi}{dz} = \alpha P_3 - \alpha\beta^2 \frac{d^2 P_3}{dz^2} + \frac{d\varphi}{dz} - 2f_1 \frac{\partial^2 w}{\partial x^2} = 0$$

$$\varepsilon_0 \frac{d^2\varphi}{dz^2} - \frac{dP_3}{dz} = 0 \tag{34}$$

$$V_{33}\Big|_{-\bar{z}_c}^{h-\bar{z}_c} = 0 \quad or \quad P_3\Big|_{-\bar{z}_c}^{h-\bar{z}_c} = 0$$

$$D_{33}\Big|_{-\bar{z}_c}^{h-\bar{z}_c} = 0 \quad or \quad \varphi\Big|_{-\bar{z}_c}^{h-\bar{z}_c} = 0 \tag{35}$$

As it is shown two equations (34) and (35) are coupled and should be solved with each other so that the function of P_3 and φ can be calculated. In this paper, for solving electric equation some boundary conditions are needed. Below boundary conditions are used as:

$$P_3 = 0 \quad at \quad z = -\bar{z}_c \quad , z = h - \bar{z}_c$$

$$D_3 = 0 \quad at \quad z = -\bar{z}_c \quad , z = h - \bar{z}_c \tag{36}$$

According to the above boundary conditions and also $\varphi(-\bar{z}_c) = 0$, electric potential and electric polarization are calculated by below equations:

$$P_3 = \frac{2f_1\varepsilon_0}{1+\alpha\varepsilon_0}\frac{\partial^2 w}{\partial x^2}\left[-\frac{e^{g\left(h-\bar{z}_c\right)} - e^{-g\bar{z}_c}}{e^{gh} - e^{-gh}} e^{-gz} - \frac{e^{-g\left(h-\bar{z}_c\right)} - e^{+g\bar{z}_c}}{e^{gh} - e^{-gh}} e^{gz} + 1 \right] \tag{37}$$

$$\varphi = \frac{2f_1\varepsilon_0}{\left(1+\alpha\varepsilon_0\right)g}\frac{\partial^2 w}{\partial x^2}\left[-\frac{e^{g\left(h-\bar{z}_c\right)} - e^{-g\bar{z}_c}}{e^{gh} - e^{-gh}} e^{-gz} + \frac{e^{-g\left(h-\bar{z}_c\right)} - e^{+g\bar{z}_c}}{e^{gh} - e^{-gh}} e^{gz} + g\left(z + \bar{z}_c\right) \right] \tag{38}$$

where $g = \sqrt{(\alpha\varepsilon_0 + 1)/(\beta^2\alpha\varepsilon_0)}$.

4. Free Vibration Analysis of Nanobeam

4.1. Free vibration formulation

In this section, formulation and free vibration analysis of functionally graded nanobeam with flexoelectric have been investigated. As it is clear, for investigating free vibration, effects of external force should be neglected. So the equations of nanobeam with boundary conditions for free vibration are shown as:

$$-\left(\frac{18}{5}l_0^2+\frac{4}{5}l_1^2\right)G_{11}\frac{\partial^5 w}{\partial x^5}+\left(\frac{18}{5}l_0^2+\frac{4}{5}l_1^2\right)D_{11}\frac{\partial^4 u_0}{\partial x^4}+B_{11}\frac{\partial^3 w}{\partial x^3}-A_{11}\frac{\partial^2 u_0}{\partial x^2}+\frac{\partial E_{11}}{\partial x}+K_{11}\frac{\partial^2 u_0}{\partial t^2}-L_{11}\frac{\partial^3 w}{\partial x\partial t^2}=0 \quad (39)$$

$$\begin{aligned}&-\left(\frac{18}{5}l_0^2+\frac{4}{5}l_1^2\right)\mathrm{H}_{11}\frac{\partial^6 w}{\partial x^6}+\left(\mathrm{C}_{11}+\left(\frac{12}{5}l_0^2+\frac{8}{15}l_1^2+2l_2^2\right)D_{11}\right)\frac{\partial^4 w}{\partial x^4}+\left(\frac{18}{5}l_0^2+\frac{4}{5}l_1^2\right)\mathrm{G}_{11}\frac{\partial^5 u_0}{\partial x^5}\\&-\mathrm{B}_{11}\frac{\partial^3 u_0}{\partial x^3}+\frac{\partial^2 F_{11}}{\partial x^2}-\frac{\partial^2 I_{11}}{\partial x^2}+K_{11}\frac{\partial^2 w}{\partial t^2}-M_{11}\frac{\partial^4 w}{\partial x^2\partial t^2}+L_{11}\frac{\partial^3 u_0}{\partial x\partial t^2}=0\end{aligned} \quad (40)$$

In these relations, coefficients are as follows:

$$\left(A_{11},B_{11},C_{11}\right)=b\int_{-\bar{z}_c}^{h-\bar{z}_c}E\left(\bar{z}\right)(1,z,z^2)dz \quad (41)$$

$$\left(D_{11},G_{11},H_{11}\right)=b\int_{-\bar{z}_c}^{h-\bar{z}_c}\mu\left(\bar{z}\right)(1,z,z^2)dz \quad (42)$$

$$\left(K_{11},L_{11},M_{11}\right)=b\int_{-\bar{z}_c}^{h-\bar{z}_c}\rho\left(\bar{z}\right)(1,z,z^2)dz \quad (43)$$

$$E_{11}=b\int_{-\bar{z}_c}^{h-\bar{z}_c}f_1\frac{dP_3}{dz}dz \quad (44)$$

$$F_{11}=b\int_{-\bar{z}_c}^{h-\bar{z}_c}f_1 z\frac{dP_3}{dz}dz \quad (45)$$

$$I_{11}=b\int_{-\bar{z}_c}^{h-\bar{z}_c}f_1 P_3 dz \quad (46)$$

4.2. Methods of solving equation

In this section, vibration solving for simply supported boundary condition has been investigated. Related boundary conditions are presented here:

$$w=w''=0 \quad ,u_0=u_0'=0 \qquad \text{at } x=0,x=L \quad (47)$$

$$\left(-M+\frac{\partial}{\partial x}\left(M^h\right)\right)=0 \qquad \text{at } x=0,x=L \quad (48)$$

For solving equations of free vibrations and calculating natural frequency, first from Eq. (39), u_0 calculated based on w and substituting in the Eq. (40). Also, time derivative of u_0 will be avoided for simplicity. So, equation of motion will reduce to one equation as follows:

$$A\frac{\partial^6 w}{\partial x^6}+\mathrm{B}\frac{\partial^4 w}{\partial x^4}+K_{11}\frac{\partial^2 \mathrm{w}}{\partial t^2}=0 \quad (49)$$

In Eq. (78), A, B values are written as:

$$A=\left(\frac{18}{5}l_0^2+\frac{4}{5}l_1^2\right)\left(\frac{G_{11}{}^2}{D_{11}}-H_{11}\right) \quad (50)$$

$$B=(C_{11}+\left(\frac{12}{5}l_0^2+2l_2^2+\frac{8}{15}l_1^2\right)D_{11}-\frac{2f_1^2\varepsilon_0 b\left(2\bar{z}_c-h\right)\left(e^{gh}-1\right)}{\left(e^{gh}+1\right)\left(\alpha\varepsilon_0+1\right)}+\frac{2f_1^2\varepsilon_0 hb}{\left(\alpha\varepsilon_0+1\right)}) \tag{51}$$

By assuming first mode function as following for simply supported boundary condition, all boundary conditions are satisfied:

$$w\left(x,t\right)=sin\left(\frac{\pi x}{L}\right)e^{i\omega t} \tag{52}$$

That ω is natural frequency of nanobeams. By substituting Eq. (80) in Eq. (78) and by using Galerkin method, natural frequency of nanobeam will be obtained.

$$\omega=\sqrt{\frac{-A}{K_{11}}\left(\frac{\pi}{L}\right)^6+\frac{B}{K_{11}}\left(\frac{\pi}{L}\right)^4} \tag{53}$$

5. Buckling Analysis of Nanobeam

By using the relations (28) to (35), equilibrium equations can be rewritten as follows:

$$-A_{11}\frac{d}{dx}\left[\frac{du_0}{dx}+\frac{1}{2}\left(\frac{dw}{dx}\right)^2\right]+B_{11}\frac{d^3w}{dx^3}+\left(\frac{18}{5}l_0^2+\frac{4}{5}l_1^2\right)\mathrm{D}_{11}\frac{\mathrm{d}^2}{\mathrm{dx}^2}\left[\frac{d^2u_0}{dx^2}+\left(\frac{dw}{dx}\right)\left(\frac{d^2w}{dx^2}\right)\right]-\left(\frac{18}{5}l_0^2+\frac{4}{5}l_1^2\right)\mathrm{G}_{11}\frac{d^5w}{dx^5}+\frac{dE_{11}}{dx}=0 \tag{54}$$

$$\begin{aligned}&\left(\frac{18}{5}l_0^2+\frac{4}{5}l_1^2\right)G_{11}\frac{d^3}{dx^3}\left[\frac{d^2u_0}{dx^2}+\left(\frac{dw}{dx}\right)\left(\frac{d^2w}{dx^2}\right)\right]-\left(\frac{18}{5}l_0^2+\frac{4}{5}l_1^2\right)H_{11}\frac{d^6w}{dx^6}\\&+\frac{d^2}{dx^2}\left\{\begin{aligned}&-B_{11}\left[\frac{du_0}{dx}+\frac{1}{2}\left(\frac{dw}{dx}\right)^2\right]+C_{11}\frac{d^2w}{dx^2}+F_{11}-I_{11}\\&+\left(\frac{12}{5}l_0^2+2l_2^2+\frac{8}{15}l_1^2\right)D_{11}\frac{d^2w}{dx^2}\\&+\left[\begin{aligned}&\left(\frac{18}{5}l_0^2+\frac{4}{5}l_1^2\right)D_{11}\left[\frac{d^2u_0}{dx^2}+\left(\frac{dw}{dx}\right)\left(\frac{d^2w}{dx^2}\right)\right]\\&-\left(\frac{18}{5}l_0^2+\frac{4}{5}l_1^2\right)G_{11}\frac{d^3w}{dx^3}\end{aligned}\right]\frac{dw}{dx}\end{aligned}\right\}+\frac{d}{dx}\left\{\begin{aligned}&\left[-A_{11}\left(\frac{du_0}{dx}+\frac{1}{2}\left(\frac{dw}{dx}\right)^2\right)+B_{11}\frac{d^2w}{dx^2}+E_{11}\right]\frac{dw}{dx}\\&+\left[\begin{aligned}&-\left(\frac{18}{5}l_0^2+\frac{4}{5}l_1^2\right)D_{11}\left(\frac{d^2u_0}{dx^2}+\left(\frac{dw}{dx}\right)\left(\frac{d^2w}{dx^2}\right)\right)\\&+\left(\frac{18}{5}l_0^2+\frac{4}{5}l_1^2\right)G_{11}\frac{d^3w}{dx^3}\end{aligned}\right]\frac{d^2w}{dx^2}\end{aligned}\right\}=0\end{aligned} \tag{55}$$

$$\alpha P_3-\alpha\beta^2\frac{d^2P_3}{dz^2}+\frac{d\varphi}{dz}-2f_1\frac{\partial^2w}{\partial x^2}=0 \tag{56}$$

$$\varepsilon_0\frac{d^2\varphi}{dz^2}-\frac{dP_3}{dz}=0 \tag{57}$$

5.1. Prebuckling analysis

In the prebuckling section, the lateral deflection must be vanished ($w^p=0$). In this case, by substituting $w^p=0$ in the equilibrium equations, all Eqs. in (54) to (57) must be satisfied. However, four equilibrium equations (54), (55), (56) and (57) will be rewritten as:

$$\alpha P_3-\alpha\beta^2\frac{d^2P_3}{dz^2}+\frac{d\varphi}{dz}=0 \tag{58}$$

$$\varepsilon_0\frac{\mathrm{d}^2\varphi}{\mathrm{dz}^2}-\frac{\mathrm{dP}_3}{\mathrm{dz}}=0 \tag{59}$$

$$\left(\frac{18}{5}l_0^2+\frac{4}{5}l_1^2\right)G_{11}\frac{d^3}{dx^3}\left[\frac{d^2u_0^{\mathrm{p}}}{dx^2}\right]-B_{11}\frac{d^2}{dx^2}\left[\frac{du_0^{\mathrm{p}}}{dx}+F_{11}-I_{11}\right]=0 \tag{60}$$

$$-A_{11}\frac{d}{dx}\left[\frac{du_0^{\mathrm{p}}}{dx}\right]+\left(\frac{18}{5}l_0^2+\frac{4}{5}l_1^2\right)\mathrm{D}_{11}\frac{\mathrm{d}^2}{\mathrm{dx}^2}\left[\frac{d^2u_0^{\mathrm{p}}}{dx^2}\right]+\frac{dE_{11}}{dx}=0 \tag{61}$$

By solving two equations (58) and (59), P_3 and φ can be obtained functionally from z. So derivative values relation to x is zero for F_{11}, I_{11}, E_{11} and can be said that Eqs. (58) and (59) will be satisfy. The other equilibrium is rewritten as:

$$-A_{11}\frac{d}{dx}\left[\frac{du_0^{\mathrm{p}}}{dx}\right]+\left(\frac{18}{5}l_0^2+\frac{4}{5}l_1^2\right)\mathrm{D}_{11}\frac{\mathrm{d}^2}{\mathrm{dx}^2}\left[\frac{d^2u_0^{\mathrm{p}}}{dx^2}\right]=0 \tag{62}$$

$$\left(\frac{18}{5}l_0^2+\frac{4}{5}l_1^2\right)G_{11}\frac{d^3}{dx^3}\left[\frac{d^2u_0^{\mathrm{p}}}{dx^2}\right]-B_{11}\frac{d^2}{dx^2}\left[\frac{du_0^{\mathrm{p}}}{dx}\right]=0 \tag{63}$$

u_0^{p} will be calculated by equations (62) and (63) with below boundary conditions.

$$\begin{gathered} u(0)=0\,,\quad \left\{+A_{11}\left[\frac{du_0^{\mathrm{p}}}{dx}\right]-\left(\frac{18}{5}l_0^2+\frac{4}{5}l_1^2\right)\mathrm{D}_{11}\frac{\mathrm{d}}{\mathrm{dx}}\left[\frac{d^2u_0^{\mathrm{p}}}{dx^2}\right]+P\right\}\Big|_{x=L}=0 \\ \left\{\left(\frac{18}{5}l_0^2+\frac{4}{5}l_1^2\right)\mathrm{D}_{11}\left[\frac{d^2u_0^{\mathrm{p}}}{dx^2}\right]\right\}\Big|_0^L=0 \end{gathered} \tag{64}$$

So, the only function of u_0^{p} that can be satisfied Eqs. (62) and (63) and boundary conditions in Eq. (64) will be calculated as:

$$u_0^{\mathrm{p}}(\mathrm{x})=\frac{-\mathrm{Px}}{\mathrm{A}_{11}} \tag{65}$$

5.2. Stability equations

According to the fact that beam will lose its stability under critical load. Achieving to critical situation is possible by applying stability equations. If the problem be bifurcation, new solution will be $u=u^p+u^i$ and $w=w^p+w^i$ and u^i and w^i are not simultaneously zero. Consequently, forces and moments will be written as [27]:

$$N=N^p+N^i\,,M=M^p+M^i\,,N^h=N^{hp}+N^{hi}\,,M^h=M^{hp}+M^{hi} \tag{66}$$

By replacing $w=w^p+w^i$ and $u=u^p+u^i$ in equilibrium equations (54) and (55), stability equations will reduced to one equation and will be written as below. It should be noted that $w^p=0$. Also second order derivative will be avoided.

$$\left(\frac{18}{5}l_0^2+\frac{4}{5}l_1^2\right)\left(\frac{G_{11}{}^2}{D_{11}}-H_{11}\right)\frac{d^6\mathrm{w}^{\mathrm{i}}}{dx^6}+(C_{11}+\left(\frac{12}{5}l_0^2+2l_2^2+\frac{8}{15}l_1^2\right)D_{11})\frac{d^4\mathrm{w}^{\mathrm{i}}}{dx^4}+\frac{d^2F_{11}}{dx^2}-\frac{d^2I_{11}}{dx^2}+\mathrm{P}\frac{d^2\mathrm{w}^{\mathrm{i}}}{dx^2}=0 \tag{67}$$

It should be noted that in above equation for simplification w instead of w^i is used.

6. Results and Discussion

In this study, functionally graded nanobeams of $BaTiO_3$ and Al_2O_3 are used, these materials used in previous researches [56, 57]. Mechanical properties of these two materials are indicated in Table (1).

Table 1. Mechanical properties of $BaTiO_3$ and Al_2O_3

Properties	Unit	Al_2O_3	$BaTiO_3$
E	GPa	390	67
μ	GPa	162.5	42.9
ρ	Kg/m^3	3960	6020

Also geometric characteristics of beam are as below:

$$L=120\,nm\,,b=10nm\,,h=8nm\,,l_0=l_1=l_2=l=0.25h \tag{68}$$

On the other hand, electric properties will be considered as constant values like below:

$$\alpha = 0.79\times10^{8}\ V.\frac{m}{C}, \varepsilon_0 = 8.85\times10^{-12}\frac{C}{V}.m\ ,\beta = 1 \tag{69}$$

In this study, Al_2O_3 as material number 1 above the beam and $BaTiO_3$ as material number 2 below the beam used as two essential materials for functionally graded nanobeam.

6.1. Validation of results

As free vibration and buckling solving of functionally graded nanobeam with flexoelectric used for the first time in this research, so there aren't any theoretical or experimental results for validation results. Therefore, in this part it is tried to validate formulation in special case $l = 0, f_1 = 0$. Validation result according to physical and mechanical properties which were investigated in Eltaher et al. [58, 59]. Table (2) shows altering the dimensionless natural frequency ($\bar{\omega} = \omega L^2\sqrt{\rho A / EI}$) by increase of power law index according to Eltaher et al's findings [58]. In this table, $L = 10000nm$, $b = 1000nm$, $h = 100nm$, $E_2 = 390Gpa, E_1 = 210Gpa$, $\rho_1 = 7800\,kg/m^3$, $\rho_2 = 3960\,kg/m^3$. Also flexoelectric and size effects have been avoided $l = 0, f_1 = 0$. In other word, there is a direct relationship between findings of these research with reference results [58]. It can be concluded that the results have a good consistency. Table (3) shows the changes of dimensionless critical force $\bar{P}_{cr} = P_{cr}L^2/EI$ with an increase of power law index according to reference [59]. In that research $L/h = 20$, $E_1 = 390Gpa$, $E_2 = 210Gpa$. This table also shows that results of this paper are more accurate than reference [59].

Table 2. Comparison of dimensionless natural frequency of simply supported nanobeam with reference [58]

	n=0	*n*=1	*n*=10
Eltaher et al. [58]	9.8797	7.0904	5.7058
Present work	9.8696	6.9963	5.6760

Table 3. Comparison of dimensionless critical load of clamped-clamped nanobeam with reference [59]

	n=0	*n*=1	*n*=10
Eltaher et al. [59]	39.4999	55.2474	66.0769
present work	39.4784	54.7058	66.4106

6.2. Changes of natural frequency and critical load with flexoelectric coefficient

By considering beam as a simply supported boundary conditions, changes of natural frequency based on changes of flexoelectric coefficient illustrated by *n*=0.5 in figure (2). In figure (3) changes of buckling critical load with flexoelectric coefficient for clamped-clamped nanobeam is shown by *n*=0.5.

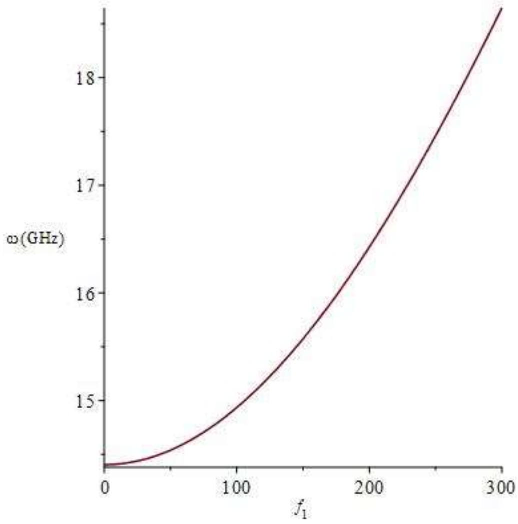

Fig. 2. Changes of natural frequency with flexoelectric coefficient for simply supported nanobeam

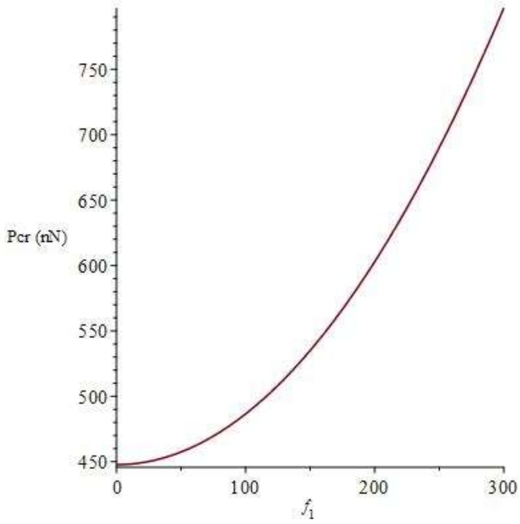

Fig. 3. Changes of critical load with flexoelectric coefficient for clamped- clamped nanobeam

As it is shown in figures (2) and (3), by increasing flexoelectric coefficient, the natural frequency and critical load will increase, It means that increase of flexoelectric coefficient leads to an increase in beam's stiffness and therefore an increase of natural frequency and critical.

6.3. Changes of natural frequency and critical load with power index

Figure (4) shows the changes of natural frequency with increase of power index for simply supported nanobeam by choosing

f_1=200. It's clear the more the index, the more beam stiffness and natural frequency. Figure (5) that's shown for f_1=200 illustrates the buckling critical load changes with power index for clamped-clamped nanobeam. It's clear that by increase of n, critical load will increase. It should be noted that, by increasing n, the stiffness of nano beam increased because the Young's modulus increased from the weaker material (E_1) to stronger material (E_2) and therefore, the natural frequency and critical buckling increased, too.

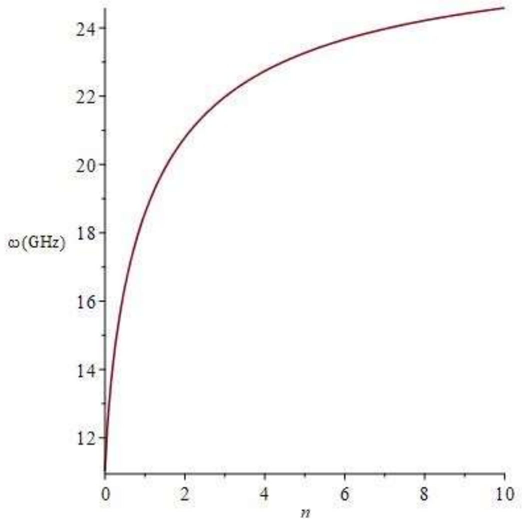

Fig. 4. Changes of natural frequency with power index for simply supported nanobeam

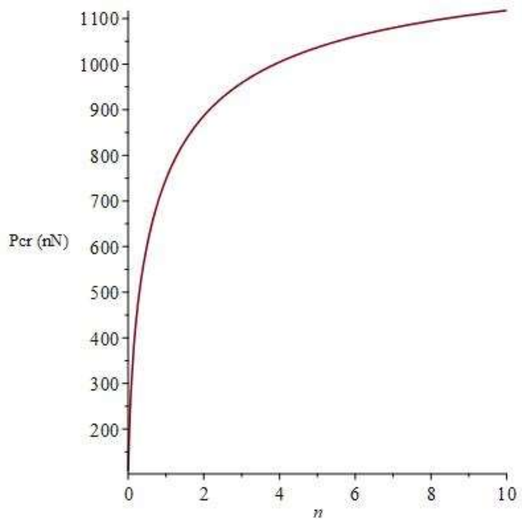

Fig. 5. Changes critical load with power index for clamped-clamped nanobeam

6.4. Changes of natural frequency and critical load with size effect

Other important note of this research is the impact of size effect on frequency and buckling critical load of this nanobeam, so that the chart of natural frequency and buckling critical load changes with regard to size effect changes are illustrated in figures (6) and (7). Figure (6) illustrated the size effect changes of l for simply supported nanobeam with $n = 0.5$ and $f_1 = 200$. It's clear that by increasing size effect, natural frequency will increase, too. Figure (7) shows the changes of critical load based on changes of size effect for clamped-clamped nanobeam. In this chart $n = 0.5$ and $f_1 = 200$. Decrease of size effect leads to the decrease of critical load.

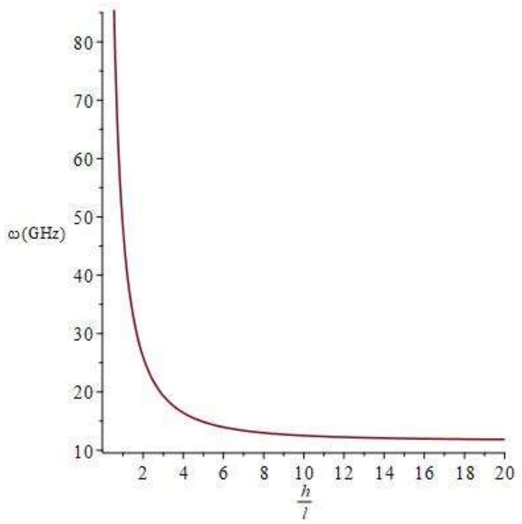

Fig. 6. changes of natural frequency with size effect for simply supported nanobeam

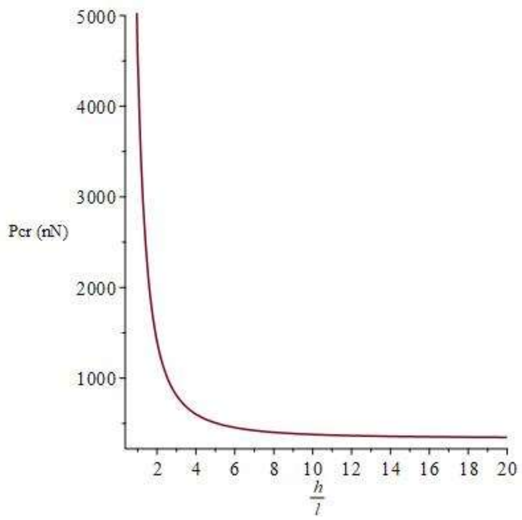

Fig. 7. changes of critical load with size effect for clamped-clamped nanobeam

As it is shown in figures (6) and (7), by increase of size effect or decrease of h/l, natural frequency and critical load will increase, it means that beam stiffness will increase. It can be concluded that size effect will increase nanobeam stiffness. According the previous research results, well-established that mechanical behaviors of micro/nano structure are size dependent. At nanoscale level, the gradient deformations vary sharply, hence the microscopic stresses and strains are not constant and depend on the shrinking length scale of the nanostructures: the smaller the structure, the more rapid the microscopic fields vary, and they do so in a way that leads to either stiffening or softening of the material. Non-classical theories based on strain gradient theory, have stiffing effect and as shown in Figs. (6) and (7) the stiffness of the nano beam increased and therefore natural frequency and critical load increased, too.

6.5. Changes of natural frequency and critical load with nanobeam geometry

Study the effect of nano beam geometry on the natural frequency was very significant. Because of nanobeam's application and their sensitivity to nano-structures, beam thickness plays an important role in designing. In figures (8) and (9), the effect of length and thickness changes of nanobeam on natural frequency is shown for simply supported nanobeam and buckling critical load for clamped –clamped nanobeam. By increasing beam length or decreasing beam thickness natural frequency and buckling critical load will decrease.

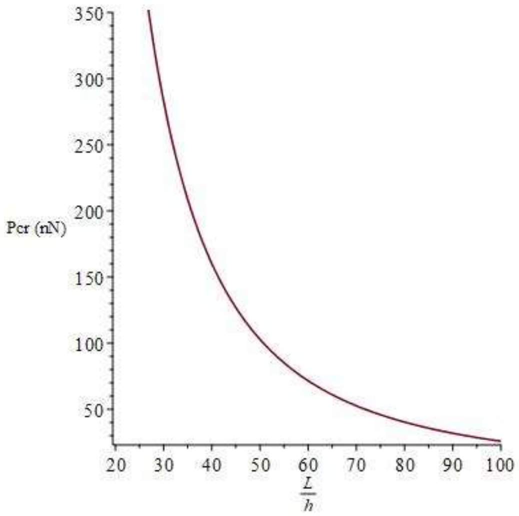

Fig. 8. changes of natural frequency with length and thickness of simply supported nanobeam

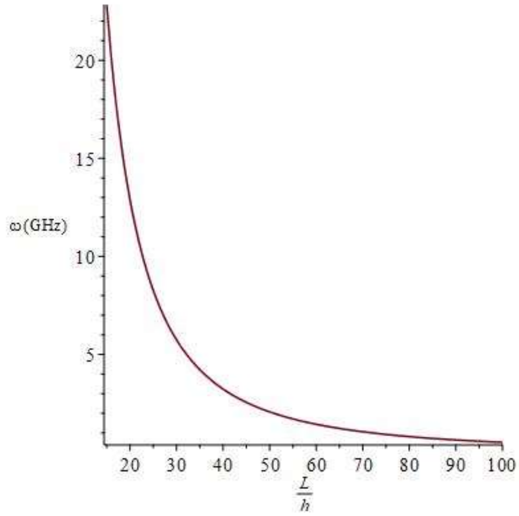

Fig. 9. changes of critical load with length and thickness of clamped- clamped nanobeam

By increasing beam thickness, natural frequency and critical load will increase. It's because of the fact that by increasing nanobeam thickness, moment of inertia will increase and consequently leads to an increase of nanobeam stiffness then, natural frequency and critical load will increase.

7. Conclusion

In this paper, nonlinear size-dependent electromechanical coupling model are developed for flexoelectric nanobeam. To achieve our goals Euler-Bernoulli beam model with presented nonclassic theory by Lee et al. [17] were used in order to derive governing equations and related boundary conditions. Then buckling and free vibration of nanobeam were investigated and some results were derived. The most important results are:

1. By increasing flexoelectric coefficient, natural frequency and buckling critical load of nanobeam will increase. This means that an increase of flexoelectric effect leads a stiffness of nanobeam incres, too.
2. By increasing power index, critical load and natural frequency will increase that has striking effect on vibrations and buckling of nanobeam.
3. By increasing size effect parameter, critical load and natural frequency will increase. It's because of the fact that size effect increase leads to increase of nanobeam stiffness. Also it shows the importance of nonclassical theories of continuum in nanobeam analysis.

Conflict of Interest

The author(s) declared no potential conflicts of interest with respect to the research, authorship and publication of this article.

Funding

The author(s) received no financial support for the research, authorship and publication of this article.

References

[1] Newell, W.E., Miniaturization of tuning forks, *Science*, 161(3848), 1968, 1320-6.
[2] Craighead, H.G., Nanoelectromechanical systems. *Science*, 290(5496), 2000, 1532-1536.
[3] Holterman, J., Groen, P., *An Introduction to piezoelectric materials and applications*, Stichting Applied Piezo, 2013.
[4] Ye, Z., *Handbook of Advanced Dielectric, Piezoelectric and Ferroelectric Materials: Synthesis, Properties and Applications*, Woodhead Publishing, 2008.
[5] Cady, W., *Piezoelectricity: an introduction to the theory and applications of electromechanical phenomena in crystals*, McGraw-Hill; 1st edition, 1946.
[6] Maranganti, R., Sharma, N.D., Sharma, P., Electromechanical coupling in nonpiezoelectric materials due to nanoscale

nonlocal size effects: Green's function solutions and embedded inclusions. *Phys. Rev. B.*, 74(1), 2006, 14110.
[7] Majdoub, M.S., Sharma, P., Cagin, T., Enhanced size-dependent piezoelectricity and elasticity in nanostructures due to the flexoelectric effect. *Phys. Rev. B.*, 77(12), 20008, 125424.
[8] Sharma, N.D., Maranganti, R., Sharma, P., On the possibility of piezoelectric nanocomposites without using piezoelectric materials. *J. Mech. Phys. Solids*, 55(11), 2007, 2328-2350.
[9] Sharma, N.D., Landis, C.M., Sharma, P., Piezoelectric thin-film superlattices without using piezoelectric materials. *J. Appl. Phys.*, 108(2), 2010, 24304.
[10] Catalan, G., Sinnamon, L.J., Gregg, J.M., The effect of flexoelectricity on the dielectric properties of inhomogeneously strained ferroelectric thin films. *J. Phys. Condens. Matter.*, 16(13), 2004, 2253-2264.
[11] Lee, D., Yoon, A., Jang, S.Y., et al. Giant Flexoelectric Effect in Ferroelectric Epitaxial Thin Films. *Phys. Rev. Lett.*, 107(5), 2011, 57602.
[12] Zhou, H., Hong, J., Zhang, Y., et al. Flexoelectricity induced increase of critical thickness in epitaxial ferroelectric thin films. *Physica B: Condensed Matter*, 407(17), 2012, 3377-3381.
[13] Eliseev, E.A., Morozovska, A.N., Glinchuk, M.D., Blinc, R., Spontaneous flexoelectric/flexomagnetic effect in nanoferroics. *Phys. Rev. B.*, 79(16), 2009, 165433.
[14] Craciunescu, C., Wuttig, M., New Ferromagnetic and Functionally Graded Shape Memory Alloys. *J. Opt. Adv. Matter.*, 5(39), 2003, 139-146.
[15] Fu, Y., Du, H., Zhang, S., Functionally graded TiN/TiNi shape memory alloy films. *Mater. Lett.*, 57(20), 2003, 2995-2999.
[16] Fu, Y., Du, H., Huang, W., Zhang, S., Hu, M., TiNi-based thin films in MEMS applications: a review. *Sens. Actuators A*, 112(2-3), 2004, 395-408.
[17] Lee, Z., Ophus, C., Fischer, L.M., et al. Metallic NEMS components fabricated from nanocomposite Al–Mo films. *Nanotechnology*, 17(12), 2006, 3063-3070.
[18] Witvrouw, A., Mehta, A., The Use of Functionally Graded Poly-SiGe Layers for MEMS Applications. Mater. Sci. Forum, 492-493, 2005, 255-260.
[19] Ma, W., Cross, L.E., Observation of the flexoelectric effect in relaxor Pb(Mg1/3Nb2/3)O3 ceramics. *Appl. Phys. Lett.*, 78(19), 2001, 2920-2921.
[20] Ma, W., Cross, L.E., Large flexoelectric polarization in ceramic lead magnesium niobate. *Appl. Phys. Lett.*, 79(26), 2001, 4420-4422.
[21] Ma, W., Cross, L.E., Flexoelectric effect in ceramic lead zirconate titanate. *Appl. Phys. Lett.*, 86(7), 2005, 72905.
[22] Ma, W., Cross, L.E., Flexoelectricity of barium titanate. *Appl. Phys. Lett.*, 88(23), 2006, 232902.
[23] Maranganti, R., Sharma, P., Atomistic determination of flexoelectric properties of crystalline dielectrics. *Phys. Rev. B.*, 80(5), 2009, 54109.
[24] Hong, J., Catalan, G., Scott, J.F., Artacho, E., The flexoelectricity of barium and strontium titanates from first principles. *J. Phys. Condens. Matter.*, 22(11), 2010, 112201.
[25] Ponomareva, I., Tagantsev, A.K., Bellaiche, L., Finite-temperature flexoelectricity in ferroelectric thin films from first principles. *Phys. Rev. B.*, 85(10), 2012, 104101.
[26] Kheibari, F., Beni, Y.T., Size dependent electro-mechanical vibration of single-walled piezoelectric nanotubes using thin shell model. *Mater., Des.*, 114, 2017, 572-583.
[27] Mehralian, F., Beni, Y.T., Ansari, R., On the size dependent buckling of anisotropic piezoelectric cylindrical shells under combined axial compression and lateral pressure. *Int. J. Mech. Sci.*, 119, 2016, 155-169.
[28] Mehralian, F., Beni, Y.T., Ansari, R., Size dependent buckling analysis of functionally graded piezoelectric cylindrical nanoshell. *Compos. Struct.*, 152, 2016, 45-61.
[29] Yue, Y.M., Xu, K.Y., Chen, T., A micro scale Timoshenko beam model for piezoelectricity with flexoelectricity and surface effects. *Compos. Struct.*, 136, 2016, 278-286.
[30] Kong, S., Zhou, S., Nie, Z., Wang, K., The size-dependent natural frequency of Bernoulli–Euler micro-beams. *Int. J. Eng. Sci.*, 46(5), 2008, 427-437.
[31] Sadeghi, H., Baghani, M., Naghdabadi, R., Strain gradient elasticity solution for functionally graded micro-cylinders. *Int. J. Eng. Sci.*, 50(1), 2012, 22-30.
[32] Yan, Z., Jiang, L., Size-dependent bending and vibration behaviour of piezoelectric nanobeams due to flexoelectricity. *J. Phys. D. Appl. Phys.*, 46(35), 2013, 355502.
[33] Liang, X., Hu, S., Shen, S., Size-dependent buckling and vibration behaviors of piezoelectric nanostructures due to flexoelectricity. *Smart. Mater. Struct.*, 24(10), 2015, 105012.
[34] Yan, Z., Jiang, L., Effect of flexoelectricity on the electroelastic fields of a hollow piezoelectric nanocylinder. *Smart. Mater. Struct.*, 24(6), 2015, 65003.
[35] Kundalwal, S.I., Megui, S.A., Effect of carbon nanotube waviness on active damping of laminated hybrid composite shells. *Acta Mech.*, 226(6), 2015, 2035-2052.
[36] Kundalwal, S.I., Suresh, Kumar, R., Ray, M.C., Smart damping of laminated fuzzy fiber reinforced composite shells using 1–3 piezoelectric composites. *Smart. Mater. Struct.*, 22(10), 2013, 105001.
[37] Suresh Kumar, R., Kundalwal, S.I., Ray, M.C., Control of large amplitude vibrations of doubly curved sandwich shells composed of fuzzy fiber reinforced composite facings. *Aerosp. Sci. Technol.*, 70, 2017, 10-28.
[38] Kundalwal, S.I., Shingare, K.B., Rathi, A., Effect of flexoelectricity on the electromechanical response of graphene nanocomposite beam, *Int. J. Mech. Mater. Des.*, 2018, https://doi.org/10.1007/s10999-018-9417-6.

[39] Kundalwal, S.I., Megui, S.A., Weng, G.J., Strain gradient polarization in graphene. *Carbon*, 117, 2017, 462-472.
[40] Chu, L., Dui, G., Ju, C., Flexoelectric effect on the bending and vibration responses of functionally graded piezoelectric nanobeams based on general modified strain gradient theory. *Compos. Struct.*, 186, 2018, 39-49.
[41] Wei, G., Shouwen, Y., Ganyun, H., Finite element characterization of the size-dependent mechanical behaviour in nanosystems. *Nanotechnology*, 17, 2016, 1118-1122.
[42] Darrall, T.B., Hadjesfandiari, A.R., Dargush G.F., Size-dependent piezoelectricity: A 2D finite element formulation for electric field-mean curvature coupling in dielectrics. *Eur. J. Mech. A. Solids*, 49, 2015, 308-320.
[43] Shijie, Z., Xie, Z., Wang, H., Theoretical and finite element modeling of piezoelectric nanobeams with surface and flexoelectricity effects. *Mech. Adv. Mater. Struct.*, 2018, https://doi.org/10.1080/15376494.2018.1432799.
[44] Soleimani, I., Beni Y.T., Vibration analysis of nanotubes based on two-node size dependent axisymmetric shell element, *Arch. Civ. Mech. Engg.*, 18, 2018, 1345–1358.
[45] Mohtashami, M., Beni Y.T., Size-Dependent Buckling and Vibrations of Piezoelectric Nanobeam with Finite Element Method. *Iran. J. Sci. Tech. Trans. Civil Engg.*, 2018, https://doi.org/10.1007/s40996-018-00229-9.
[46] Moura, A.G., Erturk, A., Electroelastodynamics of flexoelectric energy conversion and harvesting in elastic dielectrics. *J. Appl. Phys.*, 121, 2017, 064110.
[47] Liang, X., Zhang, R., Hu, S., Shen, S., Flexoelectric energy harvesters based on Timoshenko laminated beam theory. *J. Intell. Mater. Syst. Struct.*, 28(15), 2017, 2064-2073.
[48] Liang, X., Hu, S., Shen, S., Nanoscale mechanical energy harvesting using piezoelectricity and flexoelectricity. *Smart. Mater. Struct.*, 26, 2017, 035050.
[49] Deng, Q., Kammoun, M., Erturk, A., Sharma, P., Nanoscale flexoelectric energy harvesting. *Int. J. Solids Struct.*, 51, 2014, 3218-3225.
[50] Wang, K.F., Wang, B.L., Non-linear flexoelectricity in energy harvesting. *Int. J. Eng. Sci.*, 116, 2017, 88-103.
[51] Hu, S., Shen, S., Variational principles and governing equations in nano-dielectrics with the flexoelectric effect. *Sci. China Phys. Mech. Astron.*, 53(8), 2010, 1497-1504.
[52] Shen, S., Hu, S., A theory of flexoelectricity with surface effect for elastic dielectrics. *J. Mech. Phys. Solids*, 58(5), 2010, 665-677.
[53] Li, A., Zhou, S., Qi, L., Chen, X., A reformulated flexoelectric theory for isotropic dielectrics. *J. Phys. D. Appl. Phys.*, 48(46), 2015, 465502.
[54] Toupin, R.A., The Elastic Dielectric. *J. Ration. Mech. Anal.*, 5, 1956, 849-915.
[55] Kuang, Z-.B., Variational principles for generalized dynamical theory of thermopiezoelectricity. *Acta Mech.*, 203(1-2), 2009, 1-11.
[56] Beni, Y.T., Size-dependent electromechanical bending, buckling, and free vibration analysis of functionally graded piezoelectric nanobeams. *J. Intell. Mater. Syst. Struct.*, 27(16), 2016, 2199-2215.
[57] Omidian, R., Beni, Y.T., Mehralian, F., Analysis of size-dependent smart flexoelectric nanobeams. *Eur. Phys. J. Plus.*, 132(11), 2017, 481.
[58] Eltaher, M.A., Emam, S.A., Mahmoud, F.F., Free vibration analysis of functionally graded size-dependent nanobeams. *Appl. Math. Comput.*, 218(14), 2012, 7406-7420.
[59] Eltaher, M.A., Emam, S.A., Mahmoud, F.F., Static and stability analysis of nonlocal functionally graded nanobeams. *Compos. Struct.*, 96, 2013, 82-88.

Appendix A

In order to calculate $\chi_{ij}^{'}$ components, relations (19), (22) and (23) are used and the non-zero deviatoric rotation gradient components are given as:

$$\begin{aligned}
\chi_{12}^{'} &= -\frac{1}{3}\frac{\partial^2 w}{\partial x^2} \\
\chi_{21}^{'} &= -\frac{2}{3}\frac{\partial^2 w}{\partial x^2} \\
\chi_{23}^{'} &= \frac{1}{3}\left(\frac{\partial^2 u_0}{\partial x^2} - z\,\frac{\partial^3 w}{\partial x^3} + \left(\frac{\partial w}{\partial x}\right)\left(\frac{\partial^2 w}{\partial x^2}\right)\right) \\
\chi_{32}^{'} &= \frac{-1}{3}\left(\frac{\partial^2 u_0}{\partial x^2} - z\,\frac{\partial^3 w}{\partial x^3} + \left(\frac{\partial w}{\partial x}\right)\left(\frac{\partial^2 w}{\partial x^2}\right)\right)
\end{aligned} \tag{70}$$

According to relation (20), the non-zero dilatation gradient components are:

$$\gamma_1 = \frac{\partial^2 u_0}{\partial x^2} - z\,\frac{\partial^3 w}{\partial x^3} + \left(\frac{\partial w}{\partial x}\right)\left(\frac{\partial^2 w}{\partial x^2}\right),\ \gamma_3 = -\frac{\partial^2 w}{\partial x^2} \tag{71}$$

According to relation (21), the non-zero stretch gradient components are:

$$\begin{aligned}
&\eta_{111}^{(1)}=\frac{2}{5}\left(\frac{\partial^2 u_0}{\partial x^2}-z\frac{\partial^3 w}{\partial x^3}+\left(\frac{\partial w}{\partial x}\right)\left(\frac{\partial^2 w}{\partial x^2}\right)\right)\\
&\eta_{333}^{(1)}=\frac{1}{5}\left(\frac{\partial^2 w}{\partial x^2}\right)\\
&\eta_{113}^{(1)}=\eta_{131}^{(1)}=\eta_{311}^{(1)}=-\frac{4}{15}\left(\frac{\partial^2 w}{\partial x^2}\right)\\
&\eta_{122}^{(1)}=\eta_{212}^{(1)}=\eta_{221}^{(1)}=\frac{-1}{5}\left(\frac{\partial^2 u_0}{\partial x^2}-z\frac{\partial^3 w}{\partial x^3}+\left(\frac{\partial w}{\partial x}\right)\left(\frac{\partial^2 w}{\partial x^2}\right)\right)\\
&\eta_{313}^{(1)}=\eta_{331}^{(1)}=\eta_{133}^{(1)}=\frac{-1}{5}\left(\frac{\partial^2 u_0}{\partial x^2}-z\frac{\partial^3 w}{\partial x^3}+\left(\frac{\partial w}{\partial x}\right)\left(\frac{\partial^2 w}{\partial x^2}\right)\right)\\
&\eta_{223}^{(1)}=\eta_{232}^{(1)}=\eta_{322}^{(1)}=\frac{1}{15}\left(\frac{\partial^2 w}{\partial x^2}\right)
\end{aligned} \tag{72}$$

In this section, a simplification assumption is done in order to calculate electric parameter easily. According to Euler-Bernoulli model, it is assumed that electric field and polarization are only available in thickness direction $(E_1=E_2=P_1=P_2=0)$. So, from (13),(14),(15),(16), we have:

$$\sigma_{11}=E\left(\bar{z}\right)\left(\frac{\partial u_0}{\partial x}-z\frac{\partial^2 w}{\partial x^2}+\left(\frac{\partial w}{\partial x}\right)\left(\frac{\partial^2 w}{\partial x^2}\right)\right)-f_1\frac{dP_3}{dz} \tag{73}$$

$$p_3=-2\mu\left(\bar{z}\right)l_0^2\left(\frac{\partial^2 w}{\partial x^2}\right)+\left(f_1+\frac{2}{3}f_2\right)P_3 \tag{74}$$

$$p_1=2\mu\left(\bar{z}\right)l_0^2\left(\frac{\partial^2 u_0}{\partial x^2}-z\frac{\partial^3 w}{\partial x^3}+\left(\frac{\partial w}{\partial x}\right)\left(\frac{\partial^2 w}{\partial x^2}\right)\right) \tag{75}$$

$$m'_{12}=-2\mu\left(\bar{z}\right)\left(l_2^2-\frac{3}{5}l_0^2\right)\left(\frac{\partial^2 w}{\partial x^2}\right)+2f_2P_3 \tag{76}$$

$$m'_{21}=-2\mu\left(\bar{z}\right)\left(l_2^2+\frac{3}{5}l_0^2\right)\left(\frac{\partial^2 w}{\partial x^2}\right)-2f_2P_3 \tag{77}$$

$$m'_{23}=\frac{12}{5}\mu\left(\bar{z}\right)l_0^2\left(\frac{\partial^2 u_0}{\partial x^2}-z\frac{\partial^3 w}{\partial x^3}+\left(\frac{\partial w}{\partial x}\right)\left(\frac{\partial^2 w}{\partial x^2}\right)\right) \tag{78}$$

$$m'_{32}=\frac{-12}{5}\mu\left(\bar{z}\right)l_0^2\left(\frac{\partial^2 u_0}{\partial x^2}-z\frac{\partial^3 w}{\partial x^3}+\left(\frac{\partial w}{\partial x}\right)\left(\frac{\partial^2 w}{\partial x^2}\right)\right) \tag{79}$$

$$\tau_{333}^{(1)}=\frac{2}{5}\mu\left(\bar{z}\right)l_1^2\left(\frac{\partial^2 w}{\partial x^2}\right) \tag{80}$$

$$\tau_{113}^{(1)}=\tau_{131}^{(1)}=\tau_{311}^{(1)}=\frac{-8}{15}\mu\left(\bar{z}\right)l_1^2\left(\frac{\partial^2 w}{\partial x^2}\right) \tag{81}$$

$$\tau_{122}^{(1)}=\tau_{212}^{(1)}=\tau_{221}^{(1)}=\frac{-2}{5}\mu\left(\bar{z}\right)l_1^2\left(\frac{\partial^2 u_0}{\partial x^2}-z\frac{\partial^3 w}{\partial x^3}+\left(\frac{\partial w}{\partial x}\right)\left(\frac{\partial^2 w}{\partial x^2}\right)\right) \tag{82}$$

$$\tau_{313}^{(1)}=\tau_{331}^{(1)}=\tau_{133}^{(1)}=\frac{-2}{5}\mu\left(\bar{z}\right)l_1^2\left(\frac{\partial^2 u_0}{\partial x^2}-z\frac{\partial^3 w}{\partial x^3}+\left(\frac{\partial w}{\partial x}\right)\left(\frac{\partial^2 w}{\partial x^2}\right)\right) \tag{83}$$

$$\tau_{223}^{(1)}=\tau_{233}^{(1)}=\tau_{232}^{(1)}=\frac{2}{15}\mu\left(\bar{z}\right)l_1^2\left(\frac{\partial^2 w}{\partial x^2}\right) \tag{84}$$

$$\tau_{111}^{(1)}=\frac{4}{5}\mu\left(\bar{z}\right)l_1^2\left(\frac{\partial^2 u_0}{\partial x^2}-z\frac{\partial^3 w}{\partial x^3}+\left(\frac{\partial w}{\partial x}\right)\left(\frac{\partial^2 w}{\partial x^2}\right)\right) \tag{85}$$

In above relations, $\bar{z}$ is distance of arbitrary point from the bottom surface. It should be noted that in mentioned relations, E is Young's modulus. Also nonzero electric filed, higher-order electric field and the electric displacement calculated by (17), (18), and (8) as:

$$E_3 = \alpha P_3 - f_1 \frac{\partial^2 w}{\partial x^2} \tag{86}$$

$$V_{33} = \alpha\beta^2\left(\frac{dP_3}{dz}\right) - f_1\left(\frac{\partial u_0}{\partial x} - z\frac{\partial^2 w}{\partial x^2} + \left(\frac{\partial w}{\partial x}\right)\left(\frac{\partial^2 w}{\partial x^2}\right)\right) \tag{87}$$

$$D_3 = -\varepsilon_0 \frac{d\phi}{dz} + P_3 \tag{88}$$

where:

$$\beta^2 = \beta_1^2 + \beta_2^2 + \beta_3^2 \tag{89}$$

Appendix B

Eigenvalue Problem

As mentioned before, stability equation obtained by:

$$\left(\frac{18}{5}l_0^2 + \frac{4}{5}l_1^2\right)\left(\frac{G_{11}{}^2}{D_{11}} - H_{11}\right)\frac{d^6 w}{dx^6} + (C_{11} + \left(\frac{12}{5}l_0^2 + 2l_2^2 + \frac{8}{15}l_1^2\right)D_{11})\frac{d^4 w}{dx^4} + \frac{d^2 F_{11}}{dx^2} - \frac{d^2 I_{11}}{dx^2} + \mathrm{P}\frac{d^2 \mathrm{w}}{dx^2} = 0 \tag{90}$$

It should be noted that $+d^2F_{11}/dx^2 - d^2I_{11}/dx^2$ are function of d^4w/dx^4 that will be obtained by relations (37), (38), (45) and (46). Therefore, a sixth order differential equation is the result of simplification of stability equation. For solving this equation, an easier way is considered.

$$A\frac{d^6 w}{dx^6} + \mathrm{B}\frac{d^4 w}{dx^4} + \mathrm{P}\frac{d^2 \mathrm{w}}{dx^2} = 0 \tag{91}$$

In relation (91), A and B value will be written as below:

$$A = \left(\frac{18}{5}l_0^2 + \frac{4}{5}l_1^2\right)\left(\frac{G_{11}{}^2}{D_{11}} - H_{11}\right) \tag{92}$$

$$B = (C_{11} + \left(\frac{12}{5}l_0^2 + 2l_2^2 + \frac{8}{15}l_1^2\right)D_{11} - \frac{2\mathrm{f}_1^2\varepsilon_0\mathrm{b}\left(2\overline{z}_c - \mathrm{h}\right)\left(\mathrm{e}^{\mathrm{gh}} - 1\right)}{\left(\mathrm{e}^{\mathrm{gh}} + 1\right)\left(\alpha\varepsilon_0 + 1\right)} + \frac{2\mathrm{f}_1^2\varepsilon_0\mathrm{hb}}{\left(\alpha\varepsilon_0 + 1\right)}) \tag{93}$$

By forming a characteristic equation for differential equation, its exact solution is:

$$w(x) = c_1 x + c_2 + c_3 cos r_1 x + c_4 sin r_1 x + c_5 cos r_2 x + c_6 sin r_2 x \tag{94}$$

where r_1 and r_2 are:

$$r_1 = \frac{\sqrt{-2A\left(B - \sqrt{-4AP + B^2}\right)}}{2A} \quad , \quad r_2 = \frac{\sqrt{-2A\left(B + \sqrt{-4AP + B^2}\right)}}{2A} \tag{95}$$

For forming eigenvalue problem, boundary condition is needed that boundary condition will be applied for clamped-clamped beam as follows:

$$w(0) = w'(0) = w''(0) = w(L) = w'(L) = w''(L) = 0 \tag{96}$$

Therefore, there are six equations that must be satisfied as following:

$$\begin{aligned}
&1)\, c_2 + c_3 + c_5 = 0 \\
&2)\, c_1 + c_4 r_1 + c_6 r_2 = 0 \\
&3)\, -c_3 r_1^2 - c_5 r_2^2 = 0 \\
&4)\, c_1 L + c_2 + c_3 cos r_1 L + c_4 \sin r_1 L + c_5 cos r_2 L + c_6 \sin r_2 L = 0 \\
&5)\, c_1 - c_3 r_1 sin r_1 L + c_4 r_1 \cos r_1 L - c_5 r_2 sin r_2 L + c_6 r_2 \cos r_2 L) = 0 \\
&6)\, -c_3 r_1^2 cos r_1 L - c_4 r_1^2 \sin r_1 L - c_5 r_2^2 cos r_2 L - c_6 r_2^2 \sin r_2 L = 0
\end{aligned} \tag{97}$$

By forming determination of coefficient and assuming them zero, the value of critical force P_{cr} will be calculable.

Appendix C

Modeling of Functionally Graded Materials

By using simple power law, mechanical properties of functionally graded nanobeam are calculable [56]:

$$X_1(\bar{z}) = 1 - \left(\frac{\bar{z}}{h}\right)^n \quad , X_2(\bar{z}) = \left(\frac{\bar{z}}{h}\right)^n \tag{98}$$

$$F(\bar{z}) = F_1 X_1(\bar{z}) + F_2 X_2(\bar{z}) \tag{99}$$

$X(\bar{z})$ is volume fraction of main materials. So, $X_1 + X_2 = 1$ and n is power law index. It should be noted that in $n = 0$ and $n = \infty$ are phases of pure substances in upper and bottom of beam. Also F_1, F_2 are mechanical properties of (1) and (2) are above and below of beam like shear modulus μ or Young's modulus E. By substituting relations (98) and (99) in equations (41), (42) and (43), the location of neutral axis and nine other coefficient can be calculated by:

$$\bar{z}_c = \left[\frac{\frac{E_1}{2} + \frac{E_2 - E_1}{n+2}}{E_1 + \frac{E_2 - E_1}{n+1}}\right] h \tag{100}$$

$$\begin{aligned} A_{11} &= \left[E_1 + \frac{E_2 - E_1}{n+1}\right] bh \\ B_{11} &= \left[\frac{E_1}{2} + \frac{E_2 - E_1}{n+2} - \left(E_2 - E_1 + \frac{E_2 - E_1}{n+1}\right)\left(\frac{\bar{z}_c}{h}\right)\right] bh^2 \\ C_{11} &= \left[\frac{E_1}{3} + \frac{E_2 - E_1}{n+3} + \left(E_1 + \frac{E_2 - E_1}{n+1}\right)\left(\frac{\bar{z}_c}{h}\right)^2 - \left(E_1 + 2\frac{E_2 - E_1}{n+2}\right)\left(\frac{\bar{z}_c}{h}\right)\right] bh^3 \end{aligned} \tag{101}$$

$$\begin{aligned} D_{11} &= \left[\mu_1 + \frac{\mu_2 - \mu_1}{n+1}\right] bh \\ G_{11} &= \left[\frac{\mu_1}{2} + \frac{\mu_2 - \mu_1}{n+2} - \left(\mu_2 - \mu_1 + \frac{\mu_2 - \mu_1}{n+1}\right)\left(\frac{\bar{z}_c}{h}\right)\right] bh^2 \\ H_{11} &= \left[\frac{\mu_1}{3} + \frac{\mu_2 - \mu_1}{n+3} + \left(\mu_1 + \frac{\mu_2 - \mu_1}{n+1}\right)\left(\frac{\bar{z}_c}{h}\right)^2 - \left(\mu_1 + 2\frac{\mu_2 - \mu_1}{n+2}\right)\left(\frac{\bar{z}_c}{h}\right)\right] bh^3 \end{aligned} \tag{102}$$

$$\begin{aligned} K_{11} &= \left[\rho_1 + \frac{\rho_2 - \rho_1}{n+1}\right] bh \\ L_{11} &= \left[\frac{\rho_1}{2} + \frac{\rho_2 - \rho_1}{n+2} - \left(\rho_2 - \rho_1 + \frac{\rho_2 - \rho_1}{n+1}\right)\left(\frac{\bar{z}_c}{h}\right)\right] bh^2 \\ M_{11} &= \left[\frac{\rho_1}{3} + \frac{\rho_2 - \rho_1}{n+3} + \left(\rho_1 + \frac{\rho_2 - \rho_1}{n+1}\right)\left(\frac{\bar{z}_c}{h}\right)^2 - \left(\rho_1 + 2\frac{\rho_2 - \rho_1}{n+2}\right)\left(\frac{\bar{z}_c}{h}\right)\right] bh^3 \end{aligned} \tag{103}$$